J Nanopart Res (2020) 22: 120
https://doi.org/10.1007/s11051-020-04870-2

RESEARCH PAPER

Synthesizing and characterizations of one-dimensional Cu-based antibiofilm surface protective coating

Ahmad Aldhameer

Received: 14 February 2020 / Accepted: 29 April 2020 / Published online: 13 May 2020

Abstract Arc melting technique followed by top-down approach, using a high-energy ball milling technique were employed to synthesize nanocrystalline of $Cu_{50}(Zr_{50-x}Ni_x)_{50}$ ($x = 0$, 10, 20 and 30 at.%) powder particles. The end-products of the alloy powders obtained after 50 h of the ball milling time were uniform in composition and had spherical-like morphology with an average particle size of 0.75 μm in diameter. The powders, which consisted of nanocrystalline grains with an average grain size of 10 nm in diameter, were used as feedstock materials for double face coating of stainless (SUS304) sheets, using cold spraying process. The coating materials enjoyed nanocrystalline structure and uniform composition. Biofilms were grown on 20-mm^2 SUS304 sheets coated coupons inoculated with 1.5×108 CFU ml^{-1} *E. coli*. Significant biofilm inhibition was recorded in the nanoparticles coated coupons in comparison with non-coated SUS304 coupon. In conclusion, this study demonstrates that formation of biofilms can be significantly inhibited by Cu-based alloys especially in case of high (Ni) content. The inhibition of biofilm formation by nanocrystalline powders of Cu-based provides a practical approach to achieve the inhibition of biofilms formed by an emerging pathogen.

Guest Editor: Sherif El-Eskandarany

This article is part of the topical collection on *Nanotechnology in Arab Countries*

A. Aldhameer (✉)
Kuwait Institute for Scientific Research Kuwait, Kuwait City, Kuwait
e-mail: aazmi@kisr.edu.kw

Keywords Biofilm · Cu · *E. coli* · FE-HRTEM/EDS · Nanomaterials · Nanocrystalline

Introduction

THE formation of biofilms in food products or food contact surfaces leads to severe problems with regard to hygienic standards and economic losses because of food spoilage. The survival of pathogenic bacteria in the food industry that come in contact with food due to insufficient cleaning of surfaces or instruments are considered as a main problem and the main source of contamination of the end-product (Chmielewski and Frank 2003). This contamination results in the elimination of the products, economic losses and furthermore, infections if food-borne pathogens are concerned (Brooks and Flint 2008). Nanoparticles (NPs) have been considered to be excellent materials in medical application due to their size dependent chemical and physical properties. It is worth to be mentioned here that NPs are similar (and even less) on size to that most of biological molecules and structures. Such nano-sized characteristics of NPs always make them promising candidate for application in both in vivo and in vitro biomedical research.

More recently a new horizon related to the employing of NPs as antimicrobials and antibacterial agents in the area of in the food industry have shown promising results on the capability of different types of NPs (e.g., Ag, Au, Cu, CuO, MgO, Al_2O_3, TiO_2, ZnO) to kill and

resist the agglomerations of many types of bacteria (Elguindi et al. 2011 & Espitia et al. 2012).

Copper (Cu) metal and its alloys with its antimicrobial/antibacterial properties are attractive materials that can be successfully used as antibacterial surface protective coating in the medical and food industrial sectors. Like silver, Cu has long been considered to be a hygienic material. Elemental Cu, which is an essential micronutrient, required in very small amounts for survival of most aerobic organisms can be toxic and inhibit microbial growth at higher concentration (Grass et al. 2012) most of studies are focused on studying the antibacterial activities of traditional Cu-based alloys, including brass 70/30 (Cu 70%, zinc 30%), CuNi (Cu 90% and Ni 10%) and bronze alloys (Zhu et al. 2012). The aim of the study is to develop novel nanocrystalline and nanocomposite powders of Cu-based that can be used as antibiofilm surface protective coating of stainless steel (substrate) used in the food industry.

Procedures

Material preparations

Elemental Cu (99.99%) spheres with diameter ranged from 5 to 25 mm in diameter, Zr (99.99%) lumps and Ni (99.9%) wires with diameter of 3 mm were balanced to give the nominal composition of $Cu_{50}(Zr_{50-x}Ni_x)_{50}$ (x = 0, 10, 20 and 30 at.%) and placed into a Cu-hearse fixed in an arc melter (AM type provided by Edmund Bühler GmbH, Germany). The melting process, which was achieved under an argon gas atmosphere (99.999%), started by melting of pure Zr getter to remove the residual gas from the arc melter's chamber. To ensure the compositional homogeneity of the obtained alloy, the pre-alloy button was overturned and remelted for six times at an electric current ranged from 175 to 250 A. The alloy buttons were then polished by SiC abrasive (grade P-80) followed by rinsing with diluted acetone solution before starting the annealing process, which was achieved under high vacuum (10–6 bar) at 800 °C for overnight (~ 14 h). The as-annealed Cu-based master alloys (Fig. 1a) were crushed into smaller pieces, using 60-ton cold press and then disintegrated into coarse particles, using a Vibratory Disc Mill RS 200, provided by RETSCH, Germany, at a speed of 1500 rpm for 30 s. The disintegrated material particles were then sieved to separate the fine powder particles (< 100 μm in diameter) from coarse granular materials to obtain finer particles of less than 200 μm in diameter, as presented in Fig. 1c. A certain amount (50 g) of the as-separated fine powders were sealed together with fifty agate balls (15 mm in diameter) into an agate vial (500 ml in volume) inside the glove box under He gas atmosphere. The system was then mounted onto a high-energy planetary ball mill (Mono Mill PULVERISETTE 6, Fritsch, Germany) operated at room temperature with a rotation speed of 300 rpm for 50 h. The as-ball milled powders obtained after 50 h of the milling time (Fig. 1d) were used as feedstock materials for cold spraying process.

Figure 2 a displays a photo captured for the robotic system used to mountain the cold spray's gun (Fig. 2b) during the powder deposition onto a strip of a stainless steel (SUS304) sheet (200 mm × 50 mm × 0.23 mm), as shown in Fig. 2b–d. The SUS304 substrate was either fixed between two jaws, as shown in Fig. 2b or on a flat horizontal thick tool steel plate (Fig. 2d). In order to prevent any undesired grain growth of the occurred powder's grains upon applying high temperature spraying process, the cold spraying procedure was achieved at 500 °C under He carrier gas atmosphere.

The process started by feeding the coating hopper with the ball milled powders so that the powders were sprayed through an expansion nozzle (Fig. 2b) at an impact velocity ranging between 1000 and 1020 m/s. The spraying process was repeated for eight times to coat the two substrate faces under the same experimental conditions. As a result, the stainless steel sheet had an excellent thin-coat reached to about 30 μm without adhesion failures, as elucidated in Fig. 2e. The as-double faced coated stainless steel sheets were then divided into almost equal squared-like coupons with surface area of about 1 cm2, as shown in Fig. 3a. The as-divided sheets had been cut into small tetragonal-like coupons (10 mm × 10 mm × 0.23 mm) before rinsed with ethanol in an ultrasonic bath for 10 min, as shown in Fig. 3b.

Materials' characterizations

The ball-milled material powders and as-coated stainless steel sheets were characterized by means of 200 kV-field emission high-resolution transmission electron microscopy/scanning transmission electron microscopy (HRTEM/STEM) supplied by JEOL-2100F, Japan. The morphological characterizations of the powders as well

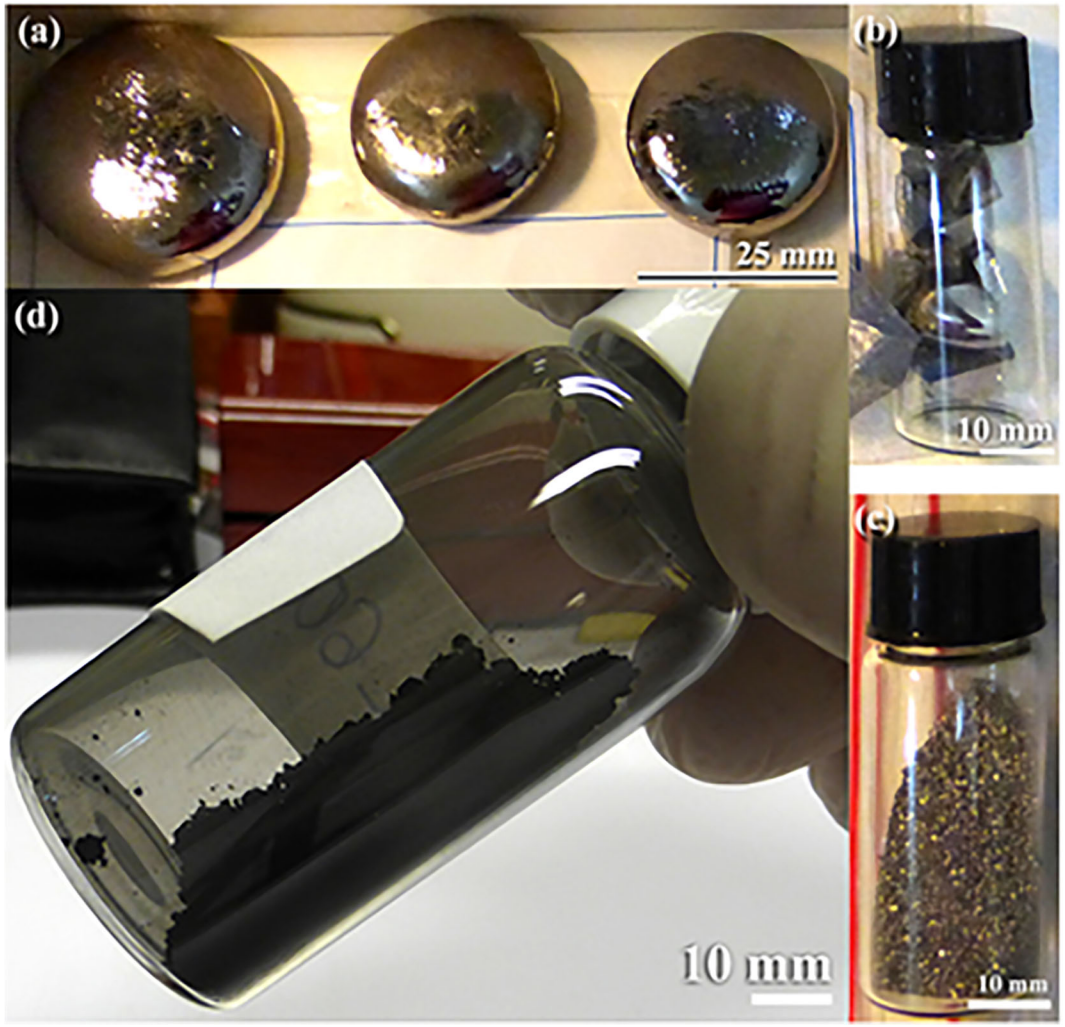

Fig. 1 **a** Synthesized buttons of as-arc melted $Cu_{50}Zr_{20}Ni_{30}$ alloys after heat treatment at 800 °C under vacuum for about 16 h, **b** pieces of as-crushed alloys, **c** as-disintegrated $Cu_{50}Zr_{20}Ni_{30}$ coarse particles, and **d** the end-product of $Cu_{50}Zr_{20}Ni_{30}$ ultrafine powders obtained after 50 h of the ball milling time

as the coating materials were investigated by 15 kV-field emission scanning electron microscope (FE-SEM, JSM-7800F, Japan). The local compositional analysis of was investigated by energy-dispersive X-ray spectroscopy (EDS, Oxford Instruments, UK) equipped with FE-SEM.

Bacterial strain and biofilm growth conditions

Biofilms were grown according to (Al-Azemi et al. 2011) with the following modifications; planktonic cells were grown in brain heart infusion (BHI) (Oxoid, UK). Biofilms were grown on 22-mm^2 coated coupons. Sterile coupons were positioned vertically in 50-ml conical tubes (BD Falcon, Franklin Lakes, NJ) with 6 ml prewarmed BHI. Tested coupons were inoculated with 100 μl 0•5 McFarland standard suspensions (equivalent to 1.5×10^8 CFU ml^{-1}) of a 24-h culture. Biofilms were left to grow for various period of time (24 h, 48 h and 72 h) at 37 °C.

Results and discussions

The micrographs of FE-SEM for the starting powders obtained upon disintegrations of as-bulk $Cu_{50}Zr_{20}Ni_{30}$ alloy and after high-energy ball milling for 50 h are shown together in Fig. 4 a and b,

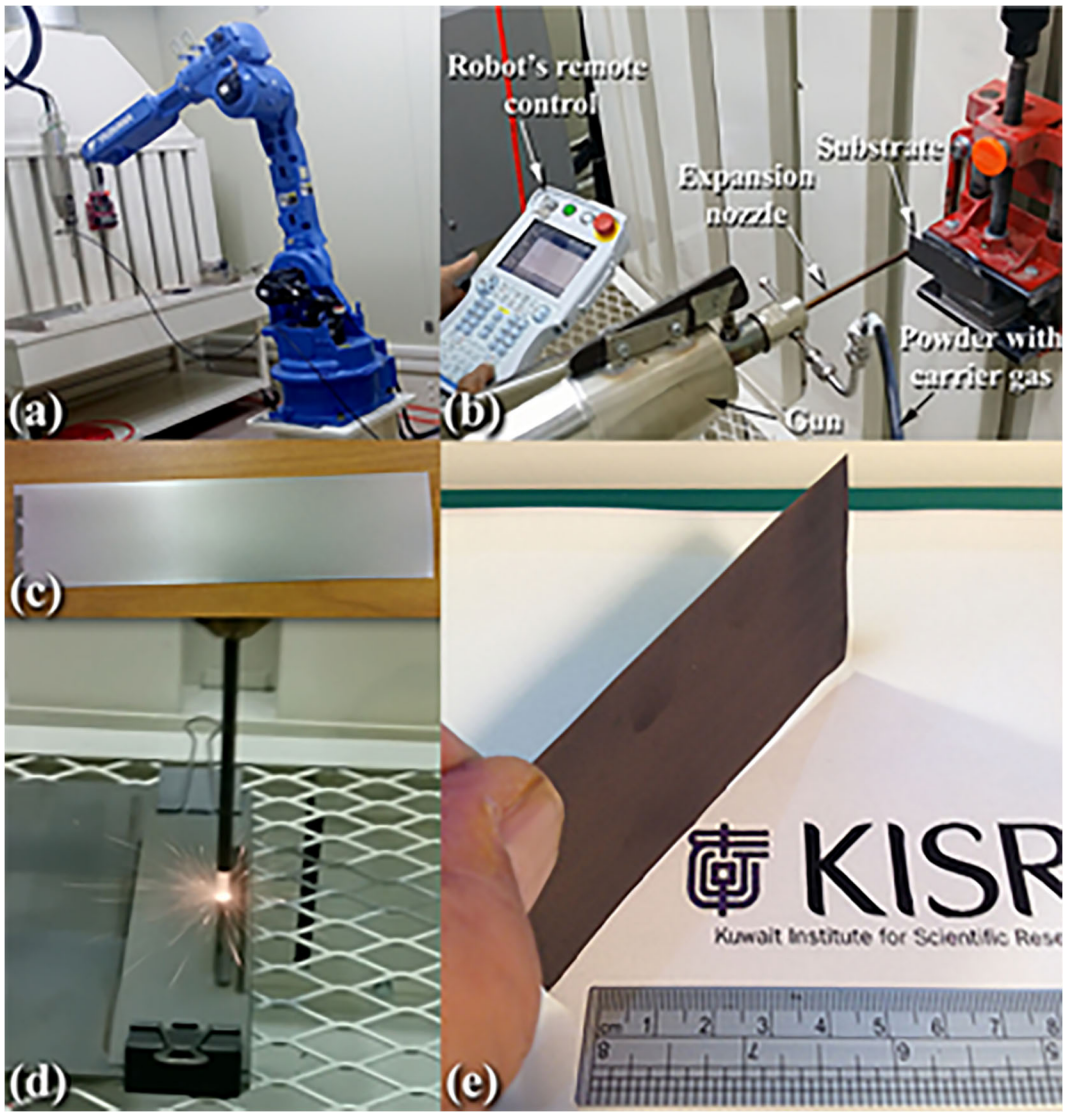

Fig. 2 Photos taken from the Nanotechnology Laboratory, Energy and Building Research Center (EBRC), Kuwait Institute for Scientific Research (KISR) of **a** the robotic system of a cold spray equipment provided by Startack Co. Ltd., **b** the components of the cold spray system, **c** an stainless steel (SUS304) sheet used in the present work as substrate, **d** the cold spraying process of the powders synthesized in the present study, and **e** the as-coated stainless sheet after completion of the spraying process

respectively. The starting materials (0 h of ball milling) had irregular particle size distribution (in the range between 20 and 180 μm in diameter) with flake-like morphology, as elucidated in Fig. 4a. Dramatic decreasing on the powder's particle sizes was achieved upon ball milling the materials for 50 h, as seen in Fig. 4b. The as-ball milled powders were enjoying smooth topology with nearly spherical-like morphology. Moreover, the particle size distribution lies in the range between 0.25 and 1 μm, as shown in Fig. 4b.

To ensure the homogeneity of the ball milled $Cu_{50}Zr_{20}Ni_{30}$ alloy powders and the elemental distribution within the sub-nano scaled, FE-SEM/EDS analysis were performed to determine both of the local composition and the elemental distribution for the as-ball milled powder materials. Figure 5 a displays the FE-SEM micrograph of an individual $Cu_{50}Zr_{20}Ni_{30}$ alloy powder particle obtained after ball milling for 50 h. The powder consisted of agglomerated fine cluster particles (~ 500 nm in diameter), as shown in Fig. 5a. The powders enjoyed were uniform in composition with the

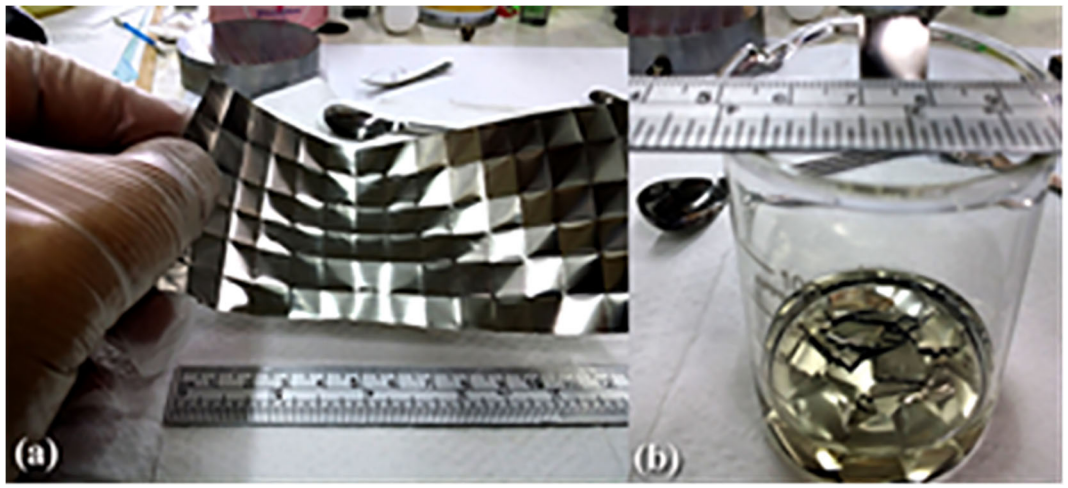

Fig. 3 Photos captured for **a** as-coated SUS304 sheet with $Cu_{50}Zr_{20}Ni_{30}$ alloy powders after simple polishing with diamond paste and then divided into equals squares with approximate dimension of 10 mm × 10 mm × 0.23 mm. The divided coupons were finally separated into individual pieces and rinsed with ethanol for 10 min (**b**)

absence of any serious degradation and/or segregation in beyond the nanoscale, indicating an excellent elemental distribution for their alloying elements of Cu (Fig. 5b, Zr (Fig. 5c) and Ni (Fig. 5d). The average composition of the calculated from at least 70 regions showed that the as-ball milled materials had very closed value ($Cu_{51}Zr_{18.5}Ni_{30.5}$) to the nominated composition of the starting $Cu_{50}Zr_{20}Ni_{30}$ alloy.

The high-resolution STEM and the atomic resolution TEM images of a selected $Cu_{50}Zr_{20}Ni_{30}$ nanopowder particle obtained after 50 h of the ball milling time are shown in Fig. 6 a and b, respectively. The nanoparticle obtained after this stage of milling was about 25 nm in diameter and had regular spherical morphology, as shown in Fig. 6a.

The HRTEM image, the indexed circular zone shown in Fig. 6a, is displayed with atomic resolution in Fig. 6b. Existence of such heavy deformations performed by the milling tools, as indicated by the staking faults shown in Fig. 6b, suggested the formation mechanism of nanocrystalline powders during high-energy ball milling of $Cu_{50}Zr_{20}Ni_{30}$ powders.

It has been demonstrated by El-Eskandarany (2015a) that the formation of nanocrystalline materials via top-down approach, using ball milling technique, is attributed to the intense cold working on the ball milled powders. This leads to a dramatic increase in the number of imperfections (e.g., point and lattice defects) which leads to decreasing the thermodynamic stability of the starting materials. Based on the type of defects applied, different kinds of nanocrystalline materials, with different physical and mechanical properties, can be obtained. It is believed that the reduction in grain size during MA takes place similar to that suggested by the model for

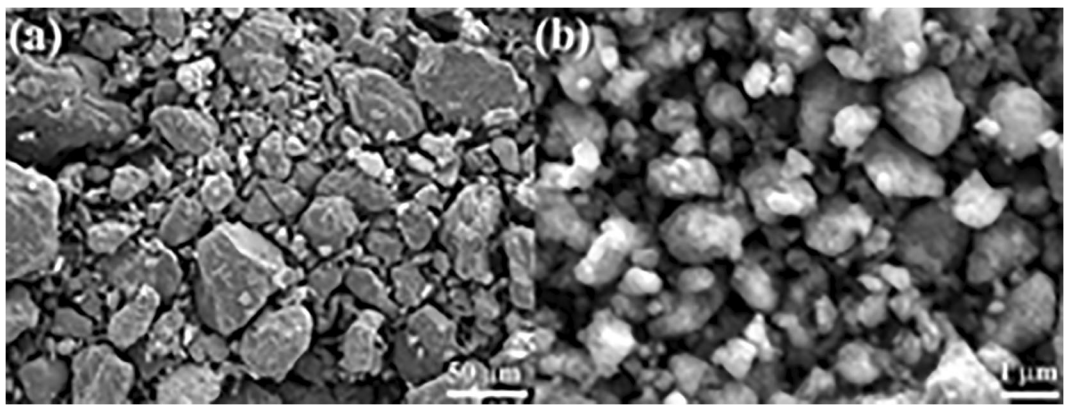

Fig. 4 FE-SEM micrographs of $Cu_{50}Zr_{20}Ni_{30}$ alloy powders obtained after ball milling for **a** 0 h and **b** 50 h

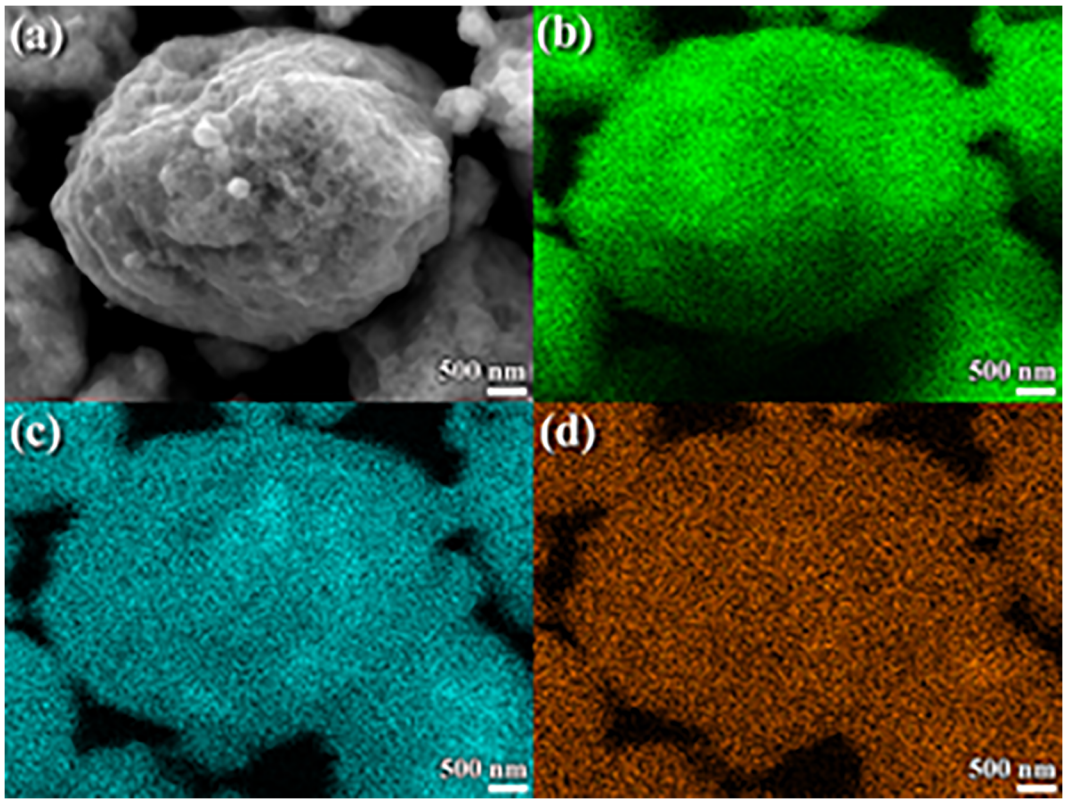

Fig. 5 a FE-SEM micrograph of $Cu_{50}Zr_{20}Ni_{30}$ alloy powder obtained after 50 h of the ball milling time and the corresponding X-ray elemental mapping for **b** Cu-Kα, **c** Zr-Kα, and **d** Ni-Kα

nanocrystalline materials fabricated by gas condensation (Birringer et al. 1984). It is worth noting that the enthalpy stored via high-energy ball milling is far above than that for the conventional cold working technique. For example, the enthalpy stored through cold welding of metals and alloys does not exceed 2 kJ/mol and is only a small fraction of the heat of fusion, ΔH_f. In the MA method, however, the enthalpy is larger and can

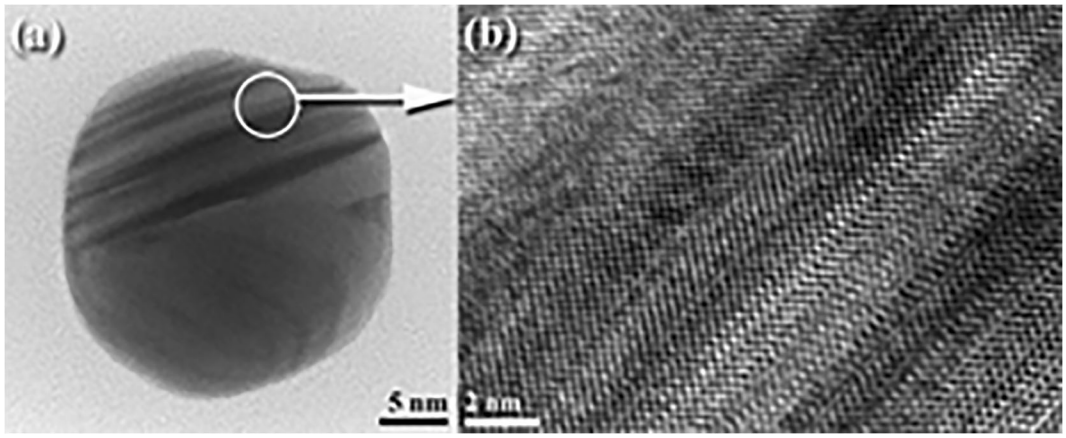

Fig. 6 **a** STEM and **b** HRTEM images of an individual nanopowder particles obtained after ball milling of $Cu_{50}Zr_{20}Ni_{30}$ alloy powder for 50 h

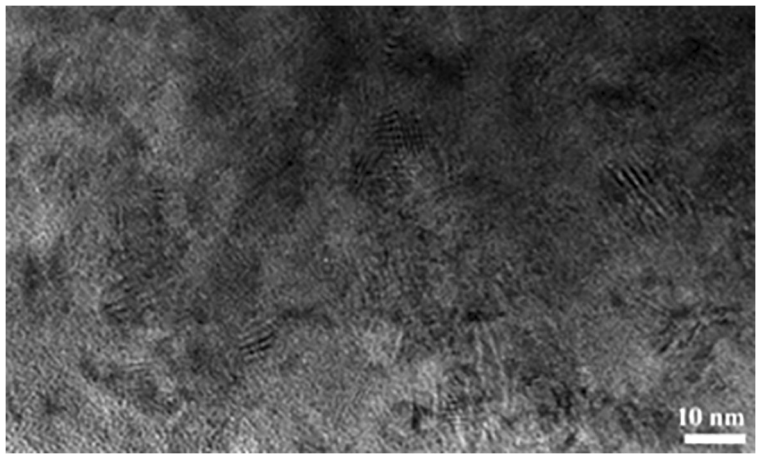

Fig. 7 HRTEM image of the cross-sectional view for as-cold prayed $Cu_{50}Zr_{20}Ni_{30}$ alloy powder deposited onto the surface of a SUS304 strip sheet at an impact velocity ranging between 1000 and 1020 m/s at 500 °C

reach higher values of crystallization enthalpies (Johnson 1986) of a metallic glass, as high as 0.4 times the heat of fusion. We should emphasize that such enthalpy storage, in the form of lattice and point defects, cannot be achieved in traditionally processed materials. Hence, the grain boundary energy of milled nanocrystalline powders is larger than the grain boundary energy of fully equilibrated grain boundary Sherif El-Eskandarany 2015b).

The atomic resolution TEM image of as-cold sprayed $Cu_{50}Zr_{20}Ni_{30}$ alloy powder deposited onto the surface of a SUS304 strip sheet is shown in Fig. 7. The coating materials consisted of nanocrystalline grains with grain sizes distributed between 8 and 28 nm in diameter, as displayed in Fig. 7. From the figure one can conclude that the cold spraying process did not lead to any severe grain growth and the coated materials enjoyed nanocrystalline properties with dense like-structure. In fact, the impact velocity gained by the sprayed powder particles upon applying the jet with a high velocity reaching to 1020 m/s led to subjecting the $Cu_{50}Zr_{20}Ni_{30}$ nanocrystalline particles under compressive stresses and this yielded to severe plastic deformation on the deposited powders. The local elemental analysis, using EDS approach showed that the cold-sprayed coating materials had uniform concentration with a minimal varying concentration limits.

Figure 8 shows the inhibitory effect of coated substrate against *E. coli* biofilm formation incubated for 24 h, 48 h and 72 h. In Fig. 8a, large amount of bacteria are observed on the control coated substrate in comparisons with SUS304 negative control; only Cu-coated substrate showed no growth. Although the inhibitory effect of Cu on biofilm formation is not well known, it is thought that Cu ion released from Cu plays an important role in alter the protein structure of bacterial cell wall. The substrates coated with $Cu_{50}Zr_{20}Ni_{30}$, $Cu_{50}Zr_{30}Ni_{20}$ and $Cu_{50}Zr_{40}Ni_{10}$ remarkably inhibited colony formation of *E. coli* compared with SUS304 (Fig. 8b, c). These results were statistically significant ($p < 0.05$). Yet not significant difference showed between other tested coated materials in comparison with SUS304. These results suggest that $Cu_{50}Zr_{20}Ni_{30}$, $Cu_{50}Zr_{30}Ni_{20}$ and $Cu_{50}Zr_{40}Ni_{10}$ coated materials will be very effective against biofilm formation in addition, results showed the improvement of antimicrobial effect of Ni when combined with Cu and Zr. It was reported that the antimicrobial effect of copper ions is dose-dependent. In our results, the pure Cu-100% significantly decreased Biofilm formation. However, antimicrobial activity was also well obtained with only Cu-50%. That may suggest synergic effect between Cu, Zr and Ni.

Conclusions

We have succeed to synthesize nanocrystalline powder particles starting from arc melting the elemental bulk materials of $Cu_{50}(Zr_{50-x}Ni_x)_{50}$ ($x = 0$, 10, 20 and 30 at.%). The Cu-based alloys were crushed and disintegrated into powder particles before subjecting to severe top-down procedure, using a room temperature ball milling technique. The as-ball milled alloy powders obtained after 50 h of ball milling had spherical-like

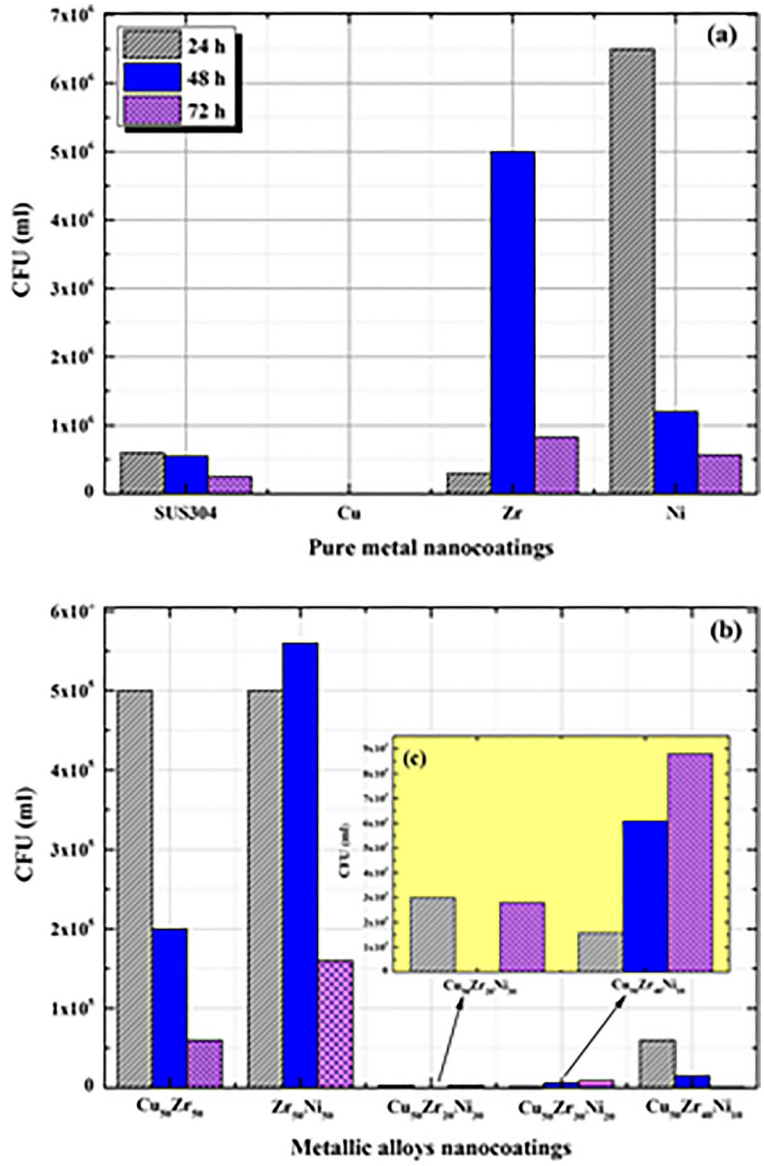

Fig. 8 Effect of metallic alloys nanocoating on biofilm formation by *E. coli* (Atcc 25,922) after 24 h, 48 h and 72 h

morphology with an average particle and grain size of 0.75 μm and 10 nm, respectively. The powder powders were used for cold spray coating of stainless (SUS304) sheets at a temperature of 500oC and powder velocity reached up to 1020 m/s processed at He gas atmosphere. The HRTEM analysis of the coating materials showed that the deposited layers maintain their nanocrystalline characteristics and the absence of any undesired grain growth and composition degradations.

Funding information This study was funded by Kuwait Institute for Scientific Research (KISR).

Compliance with ethical standards

Conflict of interest The authors declare that they have no conflict of interest.

References

Al-Azemi A, Fielder MD, Abuknesha RA, Price RG (2011) Effects of chelating agent and environmental stresses on microbial biofilms: relevance to clinical microbiology. J Appl Microbiol 110:1307–1313

Birringer R, Gleiter H, Klein HP, Marquardt P (1984) Phys Lett A 102:3423

Brooks JD, Flint SH (2008) Biofilms in the food industry: problems and potential solutions. Int J Food Sci Technol 43: 2163–2176

Chmielewski RAN, Frank JF (2003) Biofilm formation and control in food processing facilities. Compr Rev Food Sci Food Saf 2:22–32

Elguindi J, Moffitt S, Hasman H, Andrade C, Raghavan S, Rensing C (2011) Metallic copper corrosion rates, moisture content, and growth medium influence survival of copper ion-resistant bacteria. Appl Microbiol Biotechnol 89: 1963e1970

Espitia PJPN, de Soares FF, dos Coimbra JSR, de Andrade NJ, Cruz RS, Medeiros EAA (2012) Zinc oxide nanoparticles: synthesis, antimicrobial activity and food packaging applications. Food Bioprocess Technol 5:1447–1464

Grass G, Rensing C, Solioz M (2012) Metallic copper as an antimicrobial surface. Appl Environ Microbiol 77: 1541e1547

Johnson WL (1986) Thermodynamic and kinetic aspects of the crystal to glass transformation in metallic materials. Prog Mater Sci 30:81–134

Sherif El-Eskandarany M (2015a) Intermetallics 63:27

Sherif El-Eskandarany M (2015b) Mechanical alloying, second Edition: nanotechnology, materials science and powder metallurgy. Elsevier, Oxford in press

Zhu L, Elguindi J, Rensing C, Ravishankar S (2012) Antimicrobial activity of different copper alloy surfaces against copper resistant and sensitive Salmonella enteric. Food Microbiol 30:303–310